

Section 2. Chemistry

DOI:10.29013/AJT-25-5.6-24-30



SECONDARY METABOLITES OF TANACETOPSIS KARATAVIENSIS PLANT

*Dilnoza E. Dusmatova*¹, *Kambarali K. Turgunov*^{1,2},
*Bakhodir Tashkhodzhaev*¹, *Rimma F. Mukhamatkhanova*¹,
and *Ildar D. Sham'yanov*¹

¹ Acad. S.Yu. Yunusov Institute of the Chemistry of Plant Substances, Academy
of Sciences of the Republic of Uzbekistan, Tashkent, Uzbekistan,

² Turin Polytechnic University, 100095, Tashkent, Uzbekistan

Cite: *Dusmatova, D.E., Turgunov, K.K., Tashkhodzhaev, B., Mukhamatkhanova, R.F., Sham'yanov, I.D. (2025). Secondary metabolites of Tanacetopsis karataviensis plant. Austrian Journal of Technical and Natural Sciences 2024, No 5 – 6. <https://doi.org/10.29013/AJT-25-5.6-24-30>*

Abstract

As part of the ongoing study of the plant *Tanacetopsis karataviensis*, this article presents the results of the isolation of the sesquiterpene lactone ridentin and the flavonoids eupatilin and luteolin from its aerial parts. The ¹H NMR spectrum of ridentin, recorded in DMSO-*d*₆ + CCl₄, did not provide complete information on the splitting patterns and coupling constants of certain protons. The X-ray crystallographic analysis confirmed the spatial structure of ridentin, which contains a 10-membered labile germacranolide macrocycle. The macrocyclic conformation of ridentin differs from that observed in the known compound subchrysine, particularly in the *syn*-orientation of the *exo*-bonds at C14 and C15. The conditional macrocycle form of subchrysine (*udCT*) differs from the *uuCC* conformation observed in ridentin crystals. These energetically favorable conformations undergo mutual interconversion in solution at room temperature. However, the absolute configuration of the ridentin molecule, according to X-ray crystallographic data, remains 1*R*, 3*S*, 6*R*, 7*S*, with an endo double bond configuration of 4*E* in the macrocycle.

Ridentin, eupatilin and luteolin have been isolated from *Tanacetopsis karataviensis* for the first time.

Keywords: *Tanacetopsis karataviensis*, ridentin, eupatilin, luteolin, NMR spectroscopy, X-ray

1. Introduction

The genus *Tanacetopsis* (Tzvelev) Kovalevsk, belonging to the family Asteraceae, includes more than 20 species, of which 9 species grow in Uzbekistan (The Plant List. (n.d.)). *Tanacetopsis karataviensis* (Kovalevsk.) Kovalevsk. (Syn. *Cancrinia karatavica* Tzvelev, *Lepidolopsis karataviensis* (Kovalevsk.) Myrzakulov, *Tanacetum karataviense* Kovalevsk.) is a perennial plant native to Central Asia (*Tanacetopsis karataviensis* (Kovalevsk.) Kovalevsk. (n.d.). *Plantarium*:).

In traditional medicine, *Tanacetopsis karataviensis* is used as an anthelmintic agent (Dusmatova, D. E. et. al., 2021), and the chloroform fraction of its ethanol extract exhibits cytotoxic activity (Hashimova, Z. S. et. al., 2022).

Previous phytochemical studies have shown that the aerial part of *Tanacetopsis karataviensis* is a source of sesquiterpene lactones (Dusmatova, D. E. et. al., 2021; Dusmatova, D. E. et. al., 2022), as well as flavonoids and triterpenoids (Dusmatova, D. E. et. al., 2024). As part of the ongoing research on *Tanacetopsis karataviensis*, this study presents the isolation and structural determination of the sesquiterpene lactone ridentin (**1**) and the flavonoids eupatilin (**2**) and luteolin (**3**) using spectroscopic methods. The spatial structure of ridentin was established based on X-ray crystallographic analysis.

2. Experimental

2.1 Plant material

The aerial part of *Tanacetopsis karataviensis* was collected in the Jizzakh region, near the Ukhum settlement, close to Mount Beshbarmok, during the flowering period (May 2023). The species was identified by Dr. Beshko N.Yu. by comparing it with a herbarium specimen (voucher specimen No. 9341G) from the Herbarium Fund of the Institute of Botany of the Academy of Sciences of the Republic of Uzbekistan.

2.2. General methods

The melting point was determined using a Melting Point Tester (BMP-M70 model, Biobase, China). The IR spectrum was recorded on a Fourier transform spectrometer (Perkin-Elmer System 2000, KBr). The ^1H and ^{13}C NMR spectra were recorded on

a JNM-ECZ 400R NMR spectrometer at 600 MHz (internal standard TMS). For thin-layer chromatography (TLC), Sorbfil (Russia) and Whatman® UV-254 (Germany) plates were used. As a developer, iodine vapors and a solution of vanillin with sulfuric acid in absolute ethanol were applied.

2.3. Isolation of secondary metabolites 1–3

The air-dried and crushed aerial part (1.1 kg) was extracted five times with 95% ethanol, ensuring that the plant material was completely immersed in the solvent each time. The contact time for each extraction was 12 hours. The combined extracts were then concentrated under vacuum, yielding a concentrated extract (0.5 L). This extract was then fractionated using sequential liquid-liquid extraction in a separatory funnel with solvents: extraction benzene (BR-2 grade), chloroform, ethyl acetate. As a result, the following fractions were obtained: 5.4 g of the extraction benzene fraction, 28.63 g of the chloroform fraction, 14.52 g of the ethyl acetate fraction.

The chloroform fraction (28.63 g) was subjected to column chromatography using silica gel (KSK grade). From the chloroform fraction of the ethanol extract, elution fractions 116–136, obtained using a chromatographic column with a solvent system (extraction benzene-ethyl acetate, 2:1), yielded a crystalline compound **1**, beige-colored, melting point 215–218°C (ethanol).

2.3.1. Ridentin (1). IR spectrum (ν_{max} , KBr, cm^{-1}): 3305 (OH), 2913 (C-H), 2879, 1762 (C=O γ -lactone), 1668, 1643 (C=C), 1441, 1402, 1306, 1264 (C=C), 1156 (C-O), 1077, 1049, 988, 959, 977, 914, 893, 878, 813, 788, 768, 704, 633, 589, 559, 538, 507, 439.

^1H NMR (600 MHz, $\text{DMSO}-d_6 + \text{CCl}_4$, δ , ppm, J/Hz): 1.60 (1H, m, overlapped, H-8a), 1.65 (3H, s, H-15), 1.81 (1H, br. d, $J = 13.2$, H-9a), 1.89 (2H, dd, $J = 11.9, 10.8$, H-2b, 8b), 2.25 (1H, tdd, $J = 13.3, 10.8, 2.5$, H-9b), 2.79 (1H, br. s, H-7), 3.76 (1H, br. s, OH), 4.03 (1H, br. d, $J = 10.8$, H-1), 4.28 (1H, br. s, H-3), 4.42 (1H, t, $J = 9.1$, H-6), 4.72 (1H, br. s, OH), 4.75 (1H, s, H-14a), 5.05 (1H, s, H-14b), 5.24 (1H, d, $J = 9.9$, H-5), 5.46 (1H, d, $J = 3$, H-13a), 6.01 (1H, d, $J = 3$, H-13b).

^{13}C NMR (150 MHz, $\text{DMSO}-d_6 + \text{CCl}_4$, δ , ppm): 74.18 (C-1), 34.79 (C-2), 73.35 (C-3), 140.24 (C-4), 124.69 (C-5), 79.40 (C-6),

40.99 (C-7), 25.95 (C-8), 37.06 (C-9), 149.82 (C-10), 139.30 (C-11), 168.87 (C-12), 120.35 (C-13), 117.23 (C-14), 11.37 (C-15).

2.3.2. Isolation of flavonoids

The ethyl acetate extract residue (14.52 g) was mixed with silica gel in a 1:1 ratio (weight-to-weight), dried, and placed on a column with a small amount of silica gel. It was then fractionated using a polarity gradient, yielding the following subfractions: extraction benzene–ethyl acetate (1:9) (1.63 g), ethyl acetate (2.00 g), ethyl acetate–methanol (50:1) (7.03 g), and methanol (0.85 g). Further chromatographic separation of the extraction benzene–ethyl acetate (1:9) subfraction resulted in the isolation of compound **2** as yellow crystals with a melting point of 235–236 °C, while compound **3**, obtained from the ethyl acetate–methanol (50:1) subfraction, was light yellow with a melting point of 289–292 °C.

Eupatilin (**2**) and luteolin (**3**) were identified by comparing their spectral data with literature references (Mukhamatkhanova, R. F. et. al., 2017; Abduwaki, M. et. al., 2014) and by direct comparison with authentic samples.

2.4. X-ray diffraction study of compound 1

To determine the spatial structure of compound **1**, X-ray diffraction analysis was performed on its crystals. The X-ray structural experiment was performed using a Bruker D8 VENTURE dual-wavelength Mo/Cu diffractometer (Germany) (Bruker, 2021) on a prismatic crystal, using CuK α radiation ($\lambda = 1.54178\text{\AA}$). Absorption correction was applied using the Multi-Scan method (SADABS) (Krause, L. et.al., 2015). The main parameters of the X-ray structural experiment are presented in Table 1.

Table 1. Main Crystallographic Parameters and Characteristics of the X-ray Structural Experiment

MolecularFormula	C ₁₅ H ₂₀ O ₄	ρ , g/cm ³	1.260
M, g/mol	264.31	CrystalSize (mm)	0.30x0.06x0.02
SpaceGroup	P1, Z=2	ScanRange 2 θ	2.9 $\leq\theta\leq$ 69.2
a, Å	6.5504(8)	TotalReflections	3954
b, Å	7.1716(8)	Reflections with I > 2 σ (I)	1880
c, Å	15.022(2)	R ₁ (I>2 σ (I) and overall)	0.063 (0.142)
α , °	87.020(8)	wR ₂	0.155 (0.179)
β , °	88.257(8)	COOF	0.953
γ , °	81.549(8)	ResidualPeaks, eÅ ⁻³	0.21 и -0.19
V, Å ³	696.9(1)	CCDC	2441079

The structure was solved and refined using the Bruker SHELXTL Software Package (Sheldrick, G. M., 2015; Sheldrick, G. M., 2015).

All non-hydrogen atoms were refined by full-matrix least squares (on F²) in the anisotropic approximation. The hydrogen atom coordinates of hydroxyl groups were located in a Fourier map and their positions refined with $U_{\text{iso}}(\text{H}) = 1.5U_{\text{eq}}(\text{O})$. Hydrogen atoms bonded to carbon atoms were placed geometrically and refined with a riding model and $U_{\text{iso}}(\text{H}) = 1.2U_{\text{eq}}(\text{C})$ or $U_{\text{iso}}(\text{H}) = 1.5U_{\text{eq}}(\text{C})$ in case methyl group.

The X-ray crystallographic data from the experiment have been deposited at the Cambridge Crystallographic Data Centre (CCDC).

3. Results and Discussion

From the chloroform fraction of the alcoholic extract, compound **1** was isolated as beige crystals with a melting point of 215–218 °C (ethanol) from eluates 116–136 during chromatographic column elution with a mixture of extraction benzene–ethyl acetate (2:1).

In the IR spectrum of compound **1**, absorption bands characteristic of hydroxyl groups (3305 cm⁻¹), the carbonyl group of the γ -lactone cycle (1762 cm⁻¹), C=C double bonds (1668, 1643, 1264 cm⁻¹), and C-O bonds (1156 cm⁻¹) were observed.

In the ¹H NMR spectrum, recorded in a solvent mixture of DMSO-*d*₆ + CCl₄,

a three-proton singlet at 1.65 ppm corresponding to a methyl group at a double bond was observed, while the lactone proton appeared as a triplet at 4.42 ppm with a coupling constant of 9.1 Hz. The olefinic proton at C-5 produced a signal in the downfield region at 5.24 ppm with a coupling constant of 9.9 Hz. A broad one-proton doublet at 4.03 ppm ($J = 10.8$ Hz) was assigned to the geminal hydroxyl proton at C-1, while the second geminal hydroxyl proton at C-3 appeared as a broad singlet at 4.28 ppm. The protons of two exocyclic double bonds resonated in the downfield region: two protons at C-14 appeared as broad singlets at 4.75 and 5.05 ppm, while two protons of the exomethylene double bond of the γ -lactone cycle appeared as doublets at 5.46 and 6.01 ppm, each with a coupling constant of 3 Hz. The broadening of many signals, such as geminal hydroxyl protons and β -position C-H protons relative to the oxygen atom in the DMSO- d_6 + CCl_4 solution (H-1,3,7, OH), as well as other signals, may be explained by the formation of hydrogen bonds. These bonds, formed by hydroxyl protons in the donor solvent deuterated dimethyl sulfoxide, slow down proton exchange between molecules, leading to signal broadening. In the presence of the nonpolar solvent CCl_4 , these hydrogen bonds may become more dynamic, further enhancing signal broadening. CCl_4 in the DMSO- d_6 mixture can alter the solvent environment, affecting proton exchange dynamics and increasing signal broadening. Additionally, the slowed proton exchange between molecules due to hydrogen bonding contributes to chemical shift inhomogeneity and signal broadening. Thus, a combination of hydrogen bonding effects, exchange processes, and solvent interactions leads to signal broadening in the

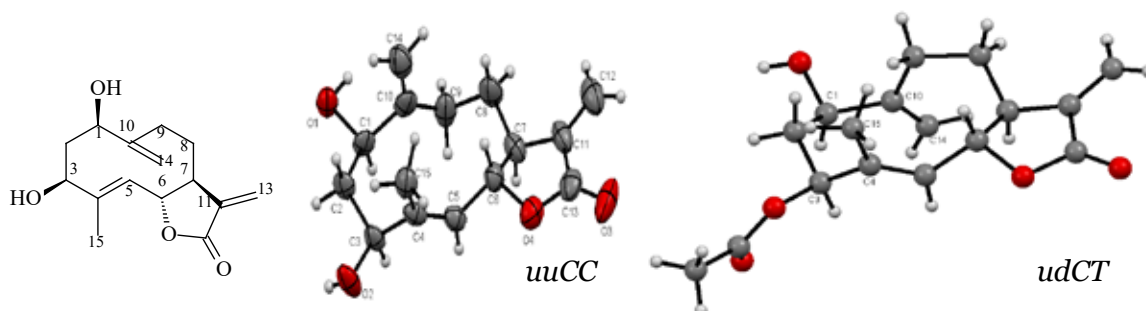
NMR spectrum. The presence of hydrogen bonds in molecule **1** was confirmed by X-ray diffraction.

The ^{13}C NMR spectrum revealed the presence of a methyl group (11.37 ppm), two hydroxyl-bearing carbons (74.18 and 73.35 ppm), a downfield-shifted γ -lactone cycle carbon bonded to oxygen, and the carbon atoms of three double bonds: 140.24 and 124.69 ppm (C5=C6); 139.30 and 120.35 ppm (C11=C13); 149.82 and 117.23 ppm (C10=C14). Additionally, the carbonyl carbon C12 was observed at 168.87 ppm.

Based on spectral data, compound **1** was identified as ridentin. Due to the limited informativeness of the ^1H NMR spectrum, its spatial structure was determined using X-ray diffraction analysis (Figure 1).

In the crystal structure of compound **1**, the asymmetric unit contains two chemically identical molecules of germacranolide lactone, designated as **1a** and **1b**. The observed bond lengths and bond angles in both molecules are identical within the experimental error margin of 3σ and do not deviate from commonly accepted values (Allen, F. H. et. al., 1987). The absolute configuration was confirmed as expected: 1*R*,3*S*,6*R*,7*S* (Fleq parameter from X-ray data: $-0.06(16)$), and the endocyclic double bond C4=C5 in the macrocycle adopts an *E*-configuration. However, molecules **1a** and **1b** exhibit slight differences in the values of the endocyclic torsional angles of the macrocycle, with deviations in some regions reaching up to 22 degrees due to the flexibility of the ten-membered macrocycle. Despite this, the overall conformational motif of the macrocycle remains consistent in both independently identified molecules. For this reason, only one of the two molecules (**1a**) is shown in Figure 1.

Figure 1. The spatial structure of ridentin (**1a**) and its 3-acetyl derivative, showing the conformational forms of the macrocycle (Kulyyasov, A. T. et. al., 1998)



According to the literature, a natural 3-*O*-acetyl derivative of ridentin, isolated from *Artemisia subchrysolepis*, is known as subchrysine (Kulyyasov, A. T. et. al., 1998). The conformation of the flexible 10-membered macrocycle in acetylridentin differs significantly from that observed in the crystal structure of compound **1**, as evidenced by visual comparison (Figure 1). As seen in Figure 1, in molecule **1**, the orientations of the exocyclic groups at C14 and C15 are *syn*-oriented, whereas in the 3-acetyl derivative, they are *anti*-oriented relative to the hypothetical plane of the 10-membered macrocycle. This

difference is also evident when comparing the endocyclic torsion angles of the macrocycle in these molecules (Table 2).

In study (Kulyyasov, A. T. et. al., 1998), the authors analyze the possible conformational minima of the 10-membered macrocycle in 3-acetylridentin, which differ by no more than 5 kcal/mol. They propose hypothetical conformational forms of the macrocycle, though these forms are not stable at room temperature in solution. According to their notation, the macrocycle in compound **1** (in our case) adopts the *uuCC* conformation.

Table 2. Endocyclic torsion angles of the macrocycle according to X-ray structural analysis (XRD)

TorsionAngles (°)	Ridentin 1a1b		Subchrysine
C1-C2-C3-C4	67	59	85.1
C2-C3-C4=C5	−109	−96	−102.2
C3-C4=C5-C6	156	162	153.1
C4=C5-C6-C7	−129	−128	−118.4
C5-C6-C7-C8	79	79	80.8
C6-C7-C8-C9	−70	−78	−49.9
C7-C8-C9-C10	95	85	−57.7
C8-C9-C10-C1	−158	−136	165.3
C9-C10-C1-C2	125	147	−53.6
C10-C1-C2-C3	−64	−82	−55.6

In crystal **1**, an intermolecular hydrogen bond O1b-H...O1a is observed between independently found molecules. The parameters of this bond are as follows: O1b...O1a distance of 2.737 Å, H...O1a distance of 1.78 Å, and O1b-H...O1a bond angle of 170°. Three additional intermolecular hydrogen bonds are formed between molecules translated along the *a* and *b* axes. The intermolecular hydrogen bonds between identical molecules O1a-H...O2a and O2b-H...O2b, translated along the *b* axis (*x*, $-1+y$, *z*), have the following hydrogen bond parameters: 2.717, 2.11, 124 and 2.787, 1.75, 163, respectively. However, molecules translated along the *a* and *b* axes ($1+x$, $1+y$, *z*) exhibit hydrogen bond parameters for O2a-H...O2b: 2.755, 2.13, 145. As a result of these intermolecular hydrogen bonds, a layer is formed in the crystal, extending along the *a* and *b* axes.

The X-ray structural analysis of ridentin was conducted for the first time.

Ridentin was previously isolated from *Artemisia giralddii* var. *giralddii* (Tan, R. X. et.al. 1999) and *A. tripartita* Rydb. ssp. *rupicola* Beetle (Irwin, M. A. et. al., 1973).

Compounds **1–3** from *Tanacetopsis karataviensis* were isolated for the first time. They are biologically active compounds. According to literature sources, ridentin exhibits antimalarial activity against *Plasmodium falciparum* FcB1 (Surowiak, A. K. et. al., 2021). Eupatilin possesses antitumor, antioxidant, anti-inflammatory, and anti-adipogenic activity (Kim, J. S. et. al., 2018; Nageen, B. et. al., 2020). Luteolin, being a widely distributed compound in flowering plants, has been well studied for its biological activity. For example, it is considered a promising candidate for the treatment of neurodegen-

erative diseases such as Parkinson's disease, Alzheimer's disease, Huntington's disease, and multiple sclerosis (Jayawickreme, D. K. et. al., 2024).

4. Conclusion

It has been revealed that *Tanacetopsis karataviensis*, a species of the flora of Uzbekistan, is a rich source of sesquiterpene lactones and flavonoids. Continuing the research, the sesquiterpene lactone ridentin was isolated for the first time from the aerial part of the plant, and its spatial structure was determined. Additionally, the flavonoids eupatilin and luteolin were identified.

The conformation of the ten-membered labile germacranolide macrocycle observed in the crystal of ridentin differs from that found in the crystal of the known germacranolide subchrysine, particularly in the mutual arrangement of the *exo*-bonds at C14 and C15.

Acknowledgments

This work was carried out with financial support from the Budgetary Program for Fundamental Scientific Research of the Institute of the Chemistry of Plant Substances, Academy of Sciences of the Republic of Uzbekistan.

References

- The Plant List. (n.d.). *The Plant List*. <http://www.theplantlist.org>
- Tanacetopsis karataviensis* (Kovalevsk.) Kovalevsk. (n.d.). *Plantarium: Plants and lichens of Russia and neighboring countries*. URL: <https://www.plantarium.ru/lang/en/page/view/item/37327.html>
- Dusmatova, D. E., Bobakulov, K. M., Mukhamatkhanova, R. F., Turgunov, K. K., Terenteva, E. O., Tsay, E. A., Sham'yanov, I. D., Tashkhodzhaev, B., Azimova, S. S., & Abdullaev, N. D. (2021). Isolation of cytotoxic sesquiterpene lactones from *Tanacetopsis karataviensis* (Kovalevsk.) Kovalevsk. *Natural Product Research*, – 35(12). – 1939 p. URL: <https://doi.org/10.1080/14786419.2019.1647423>
- Hashimova, Z. S., Dusmatova, D. E., Terentyeva, E. O., Tsai, E. A., Mukhamatkhanova, R. F., Shamyaynov, I. D., & Azimova, Sh. S. (2022). Patent No. IAP 06877. Tashkent, Uzbekistan: Agency for Intellectual Property under the Ministry of Justice of the Republic of Uzbekistan. (In Russian).
- Dusmatova, D. E., Bobakulov, Kh. M., Turgunov, K. K., Mukhamatkhanova, R. F., Uzbekov, V. V., Gildenast, H., Englert, U., Sham'yanov, I. D., Tashkhojaev, B., Bruskov, V. P., & Abdullaev, N. D. (2022). Guaianolides from *Tanacetopsis karataviensis*. *Natural Product Research*, – 36(11). – 1734 p. URL: <https://doi.org/10.1080/14786419.2020.1813137>
- Dusmatova, D. E., Mukhamatkhanova, R. F., Levkovich, M. G., Okhundedaev, B. S., Sham'yanov, I. D., Akhmedov, V. N., Akhmedova, Z. Yu., & Abdullaev, N. D. (2024). Constituents of *Tanacetopsis karataviensis*. *Chemistry of Natural Compounds*, – 60. – 180 p. URL: <https://doi.org/10.1007/s10600-024-04283-w>
- Mukhamatkhanova, R. F., Bobakulov, Kh. M., Sham'yanov, I. D., & Abdullaev, N. D. (2017). Flavonoids of *Artemisia tenuisecta*. *Chemistry of Natural Compounds*, – 53. – 750 p. URL: <https://doi.org/10.1007/s10600-017-2109-x>
- Abduwaki, M., Eshbakova, K. A., Dong, J. C., & Aisa, H. A. (2014). Flavonoids from flowers of *Hyssopus cuspidatus*. *Chemistry of Natural Compounds*, – 50. – 915 p. URL: <https://doi.org/10.1007/s10600-014-1116-4>
- Bruker. (2021). *APEX4* (Software). Bruker AXS Inc.
- Krause, L., Herbst-Irmer, R., Sheldrick, G. M., & Stalke, D. (2015). Comparison of silver and molybdenum microfocus X-ray sources for single-crystal structure determination. *Journal of Applied Crystallography*, – 48(1). – 3 p. URL: <https://doi.org/10.1107/S1600576714022985>
- Sheldrick, G. M. (2015). SHELXT – Integrated space-group and crystal-structure determination. *Acta Crystallographica Section A*, – 71(1). – 3. URL: <https://doi.org/10.1107/S2053273314026370>

- Sheldrick, G. M. (2015). Crystal structure refinement with SHELXL. *Acta Crystallographica Section C*, – 71(1). – 3 p. URL: <https://doi.org/10.1107/S2053229614024218>
- Allen, F. H., Kennard, O., Watson, D. G., Brammer, L., Orpen, A. G., & Taylor, R. (1987). Tables of bond lengths determined by X-ray and neutron diffraction. Part 1. Bond lengths in organic compounds. *Journal of the Chemical Society, Perkin Transactions – 2*, – 1 p. URL: <https://doi.org/10.1039/P298700000S1>
- Kulyyasov, A. T., Bagryanskaya, I. Yu., Gatilov, Yu. V., Shakirov, M. M., Raldugin, V. A., Ađenov, S. M., & Seitembetov, T. S. (1998). Crystal and molecular structure of subchrysine (3-O-acetylridentine), a new germacranolide from *Artemisia subchrysolepis*. *Russian Chemical Bulletin*, – 47. – 1390 p. URL: <https://doi.org/10.1007/BF02495573>
- Tan, R. X., Lu, H., Wolfender, J. L., Yu, T. T., Zheng, W. F., Yang, L., Gafner, S., & Hostettmann, K. (1999). Mono- and sesquiterpenes and antifungal constituents from *Artemisia* species. *Planta Medica*, – 65(1). – 64 p. URL: <https://doi.org/10.1055/s-1999-13965>
- Irwin, M. A., & Geissman, T. A. (1973). Ridentin B: an eudesmanolide from *Artemisia tripartita* ssp. *rupicola*. *Phytochemistry*, – 12(4). – 871 p. URL: [https://doi.org/10.1016/0031-9422\(73\)80693-4](https://doi.org/10.1016/0031-9422(73)80693-4)
- Surowiak, A. K., Balcerzak, L., Lochynski, S., & Strub, D. J. (2021). Biological activity of selected natural and synthetic terpenoid lactones. *International Journal of Molecular Sciences*, – 22(9). – 5036 p. URL: <https://doi.org/10.3390/ijms22095036>
- Kim, J. S., Lee, S. G., Min, K., Kwon, T. K., Kim, H. J., & Nam, J. O. (2018). Eupatilin inhibits adipogenesis through suppression of PPAR γ activity in 3T3-L1 cells. *Biomedicine & Pharmacotherapy*, – 103. – 135 p. URL: <https://doi.org/10.1016/j.biopha.2018.03.073>
- Nageen, B., Sarfraz, I., Rasul, A., Hussain, G., Rukhsar, F., Irshad, S., Riaz, A., Selamoglu, Z., & Ali, M. (2020). Eupatilin: A natural pharmacologically active flavone compound with its wide range applications. *Journal of Asian Natural Products Research*, – 22(1). – P. 1–20. URL: <https://doi.org/10.1080/10286020.2018.1492565>
- Jayawickreme, D. K., Ekwosi, C., Anand, A., Andres-Mach, M., Wlaź, P., & Socała, K. (2024). Luteolin for neurodegenerative diseases: A review. *Pharmacological Reports*, – 76. – 644 p. URL: <https://doi.org/10.1007/s43440-024-00610-8>

submitted 16.06.2025;

accepted for publication 30.06.2025;

published 31.07.2025

© Dusmatova, D. E., Turgunov, K. K., Tashkhodzhaev, B., Mukhamatkhanova, R. F., Sham'yanov, I. D.

Contact: doctor.dusmatova@mail.ru